Vol 15 No 8, August 2006
1009-1963/2006/15(08)/1843-06

Chinese Physics

© 2006 Chin. Phys. Soc.
and IOP Publishing Ltd

Accurate evaluation of lowest band gaps in ternary locally resonant phononic crystals*

Wang Gang(王　刚)[a)b)†], Shao Li-Hui(邵丽晖)[c)],
Liu Yao-Zong(刘耀宗)[a)b)], and Wen Ji-Hong(温激鸿)[a)b)]

[a)] *Institute of Mechatronical Engineering, National University of Defense Technology, Changsha* 410073,*China*

[b)] *Photonic/Phononic Band Gap Research Center, National University of Defense Technology, Changsha* 410073,*China*

[c)] *Astronaut Center of China, Beijing* 100094, *China*

(Received 16 September 2005; revised manuscript received 29 April 2006)

Based on a better understanding of the lattice vibration modes, two simple spring–mass models are constructed in order to evaluate the frequencies on both the lower and upper edges of the lowest locally resonant band gaps of the ternary locally resonant phononic crystals. The parameters of the models are given in a reasonable way based on the physical insight into the band gap mechanism. Both the lumped-mass methods and our models are used in the study of the influences of structural and the material parameters on frequencies on both edges of the lowest gaps in the ternary locally resonant phononic crystals. The analytical evaluations with our models and the theoretical predictions with the lumped-mass method are in good agreement with each other. The newly proposed heuristic models are helpful for a better understanding of the locally resonant band gap mechanism, as well as more accurate evaluation of the band edge frequencies.

Keywords: phononic crystals, locally resonant, analog model
PACC: 4320, 4335, 0260, 8160H

1. Introduction

In recent years, a great deal of work has been devoted to the study of the propagation of elastic or acoustic wave in periodic structures composed of different materials,[1−16] which are referred to as the phononic crystals (PCs)[1] by analogy with the photonic crystals[17,18] for electromagnetic waves. Because of the periodicity in such structures, there exist frequency ranges in which elastic waves are forbidden. This phenomenon can be of real interest because of the rich physics of elastic system, where the wave can mix longitudinal modes with transverse modes and a large contrast between the elastic parameters is allowed as well. A well-known example is the locally resonant (LR) PCs consisting of very soft rubber[2,5] (with an elastic constant of five orders lower than that of common solids) and other components. These new materials are most likely to obtain the low-frequency gaps with structures of small dimensions, leading to promising applications such as low-frequency vibration/noise insulations.

The lumped-mass (LM) method is employed in the study of two-dimensional (2D) and three-dimensional (3D) ternary LR PCs in this paper, firstly proposed in the 1D form[9] and recently extended to two-[11,13] and three-dimensional forms. The method is based on the idea of the discretization of the continuous system. It has been concluded[11,13] that the LM method converges faster than the traditional techniques and its convergence is insensitive to the sharp variation in elastic constant on the interfaces inside PCs. Moreover, it can be easily used in the band gap calculation of PCs with complex lattice structures. These advantages are unique in comparison with the other work[5,14] on the improvement of traditional methods.

Several analogous models have been used in the research of the mechanism of low-frequency band gaps in the LR PCs.[5−7,12] A simple mechanical model of mass and spring was first used by Goffaux, *et al* [5,6] in order to fit the transmission spectra near the first resonant peak and the edges of the first band gaps in a 2D ternary LR PCs. We also establish a similar model in order to clarify the origin of the LR band gaps in 2D binary LR PCs.[12] However, the parameters of these models[5,6,12] are given, not calculated with a reasonable method based on physical insights.

*Project supported by the National Natural Science Foundation of China (Grant No 50575222) and the State Key Development Program for Basic Research of China (Grant No 51307).
†E-mail: wang-g@vip.sina.com

Hirsekorn used a different simple model[7] to evaluate the frequencies on the lower edges of the band gaps in 2D ternary LR PCs, and a reasonable derivation of the parameters in the model is given. However, the thin rubber layers in arc shape are treated as simple equal-thickness flat layers in his model,[7] and the model can be used only to simulate the lower edges of the band gaps with slight mismatches. But Hirsekorn's work[7] does motivate the present study.

Here, in order to study the origin of the LR band gaps more sufficiently, we restudy the lattice vibration modes that are related to the formation of the lowest LR band gaps of typical[2] ternary PCs with the LM method. An additional analogous model is constructed to represent the vibration modes on the upper edges of the LR band gaps. The parameters of the two models are calculated based on a clear understanding of the physical insight. The two models and the arithmetic of its parameters are verified with the LM method by changing the structural and material parameters of the ternary LR PCs.

2. Lattice vibration modes of the ternary LR PCs

Figure 1 illustrates the band structure of typical 3D ternary LR PCs[2] that is composed of simple cubic arrays of coated Pb spheres immersed in epoxy. Figure 2 illustrates the lattice vibration modes corresponding to points $L_{1,2,3}$, $L_{4,5,6}$ and $L'_{4,5,6}$ in Fig.1.

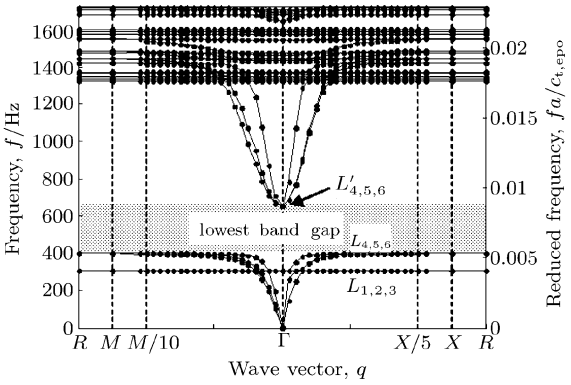


Fig.1. The band structure of typical 3D[2] ternary LR PCs calculated with the 3D LM method. The shadowed region represents the lowest band gap.

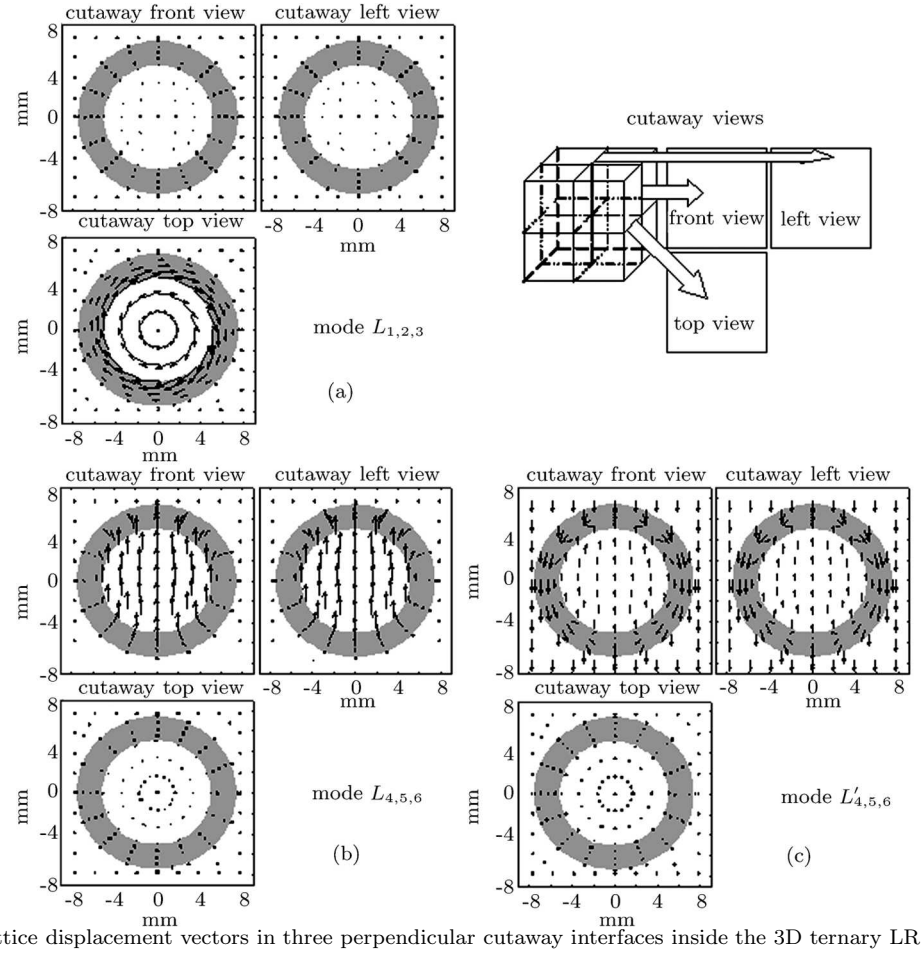


Fig.2. Lattice displacement vectors in three perpendicular cutaway interfaces inside the 3D ternary LR PCs corresponding to (a) $L_{1,2,3}$, (b) $L_{4,5,6}$ and (c) $L'_{4,5,6}$ in Fig.1 respectively. The direction and the length of each arrow represent the direction and amplitude of the displacement vector at the starting point of the arrow. The shadowed region, the inside and the outside represent the coating rubber, Pb core and epoxy host respectively.

Similar to the case of 2D ternary LR PCs,[10] Fig.3(a) illustrates a clockwork-like torsion LR mode that cannot generate a gap.[10] However, The lowest LR band gaps in 3D ternary LR PCs are generated by the 4–6th LR modes $L_{4,5,6}$ that are combined together and illustrated in Fig.2(b), where the core vibrates as a rigid sphere and the coating acts as springs. Dynamic balance of the whole system is insured by the fixed delay in phase of adjacent lattices. As to the other three vibration modes at points $L'_{4,5,6}$ in Fig.1 that are illustrated in Fig.2(c) (on the upper edge of the lowest band gap), the host media vibrates with an opposite phase to the core. The synchronous vibration of the whole system insures the dynamic balance.

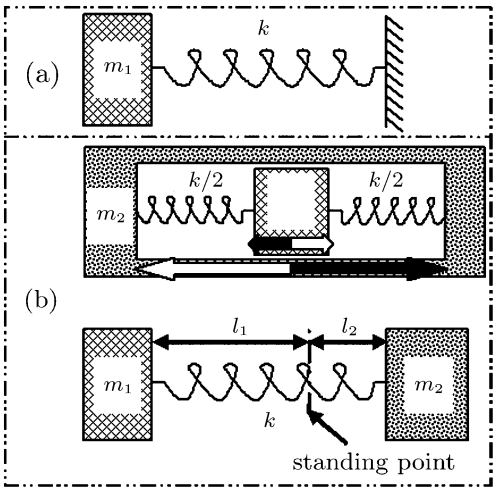


Fig.3. Analogous models corresponding to vibration modes on the (a) lower and (b) upper edges of the lowest LR band gap.

The corresponding lattice vibration modes of the 2D LR PCs have been discussed partly before.[10] As the lattice vibration modes are similar to those in the corresponding 3D case, they are elided in this paper.

3. Analogous models and the calculation of relevant parameters

Based on the above discussion, we can conclude as follows.

1) The vibration modes on the lower edges of the lowest band gaps in both the 2D and the 3D LR PCs correspond to the mass–spring model illustrated in Fig.3(a). In the model, particles m_1 represents the equivalent mass of one oscillator and spring k represents the equivalent stiffness of the oscillator.

2) The vibration modes on the upper edges of the lowest band gaps in both the 2D and the 3D LR PCs can be described with a new 'mass–spring–mass' model illustrated in Fig.3(b). In the model, the new particles m_2 represents the equivalent mass of host media in a lattice.

As the phenomena in the 2D and 3D ternary LR PCs around the lowest band gaps can be easily described with the sample models in Fig.3, they may be used to evaluate the frequencies on the edges of the lowest band gap. This evaluation is very helpful for the simplification of the design of the LR PCs. However, accurate evaluations need the correct calculations of the parameters in the analogous models. Here, three calculation methods are used and compared in the evaluation of frequencies of the lowest band gaps in 2D and 3D ternary LR PCs.

Based on the detailed vibration modes illustrated in Fig.2, we can see that only rubbers in region A (illustrated in Fig.4) are mainly compressed and stretched when the core vibrates up and down. So stiffness k in Fig.3 can be calculated with parameters in region A.

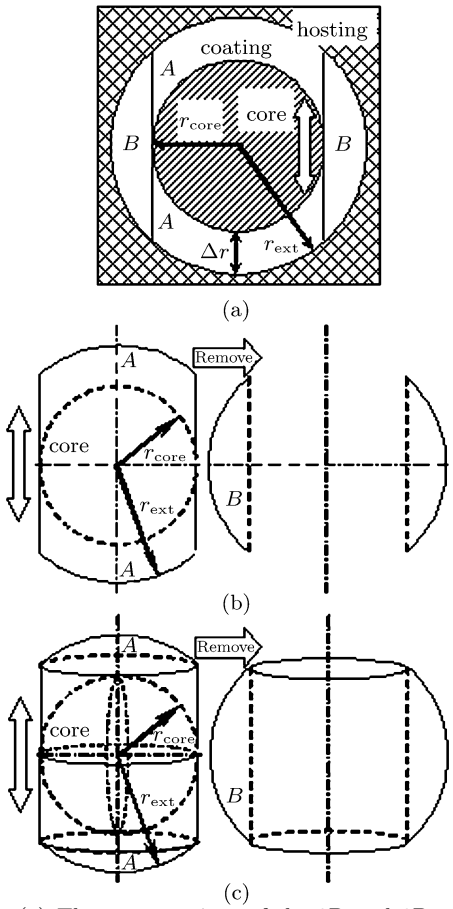


Fig.4. (a) The cross sections of the 2D and 3D ternary LR PCs. (b) and (c) Sketch maps explaining the calculation methods of parameters in the analogous models corresponding to 2D and 3D ternary LR PCs respectively.

Firstly, Hirsekorn's method[7] is used as method I in this paper. In method I, the m_1 and m_2 in Fig.3

are calculated with the mass of the core and epoxy host in a lattice respectively, and the rubber in region A is treated as two layers with equal-thickness Δr for simplicity. Thus, for the typical 2D ternary LR PC, we have

$$m_1 = m_{\text{core}} = \rho_{\text{core}} \pi r_{\text{core}}^2, \tag{1}$$

$$m_2 = m_{\text{host}} = \rho_{\text{host}} (a^2 - \pi r_{\text{ext}}^2), \tag{2}$$

$$k = \frac{4C_{11} r_{\text{core}}}{r_{\text{ext}} - r_{\text{core}}}, \tag{3}$$

and for the typical 3D one,

$$m_1 = m_{\text{core}} = \frac{4}{3} \rho_{\text{core}} \pi r_{\text{core}}^3, \tag{4}$$

$$m_2 = m_{\text{host}} = \rho_{\text{host}} (a^3 - \frac{4}{3} \pi r_{\text{ext}}^3), \tag{5}$$

$$k = \frac{2C_{11} \pi r_{\text{core}}^2}{r_{\text{ext}} - r_{\text{core}}}, \tag{6}$$

where $C_{11} = \lambda_{\text{coating}} + 2\mu_{\text{coating}}$; $\lambda_{\text{coating}}$and μ_{coating} are the Lame constants of the rubber in the coating layer.

With the two models illustrated in Fig.3, the frequencies on the edges of the lowest LR band gap can be evaluated with

$$f_1 = \frac{1}{2\pi} \sqrt{\frac{k}{m_1}};\ f_2 = \frac{1}{2\pi} \sqrt{\frac{k(m_1 + m_2)}{m_1 m_2}}. \tag{7}$$

Using method I and the model in Fig.3, we evaluate the frequencies of the lowest band gap of the typical 3D ternary LR PCs with different structural and material parameters (dotted lines in Figs.5–9) and compared them with that calculated with the LM method (solid lines with dots in Figs.5–9).

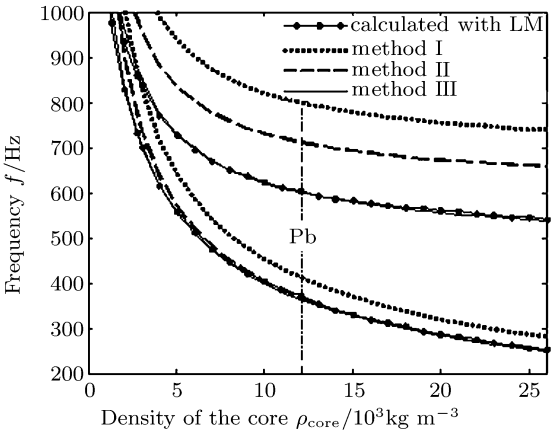


Fig.5. Frequencies on the edges of the lowest band gaps in the typical 3D ternary LR PCs at several densities of the core.

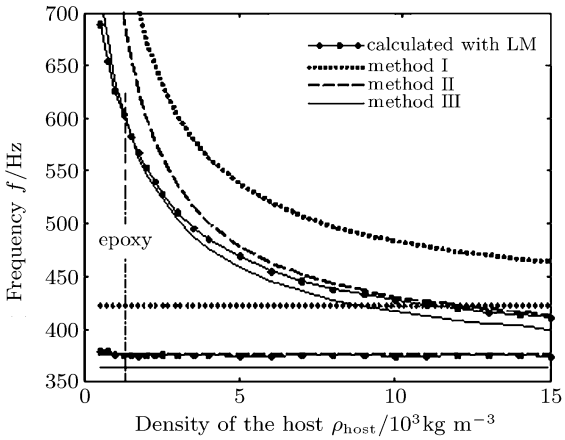


Fig.6. Frequencies on the edges of the lowest band gaps in the typical (a)2D and (b)3D ternary LR PCs at several densities of the host material.

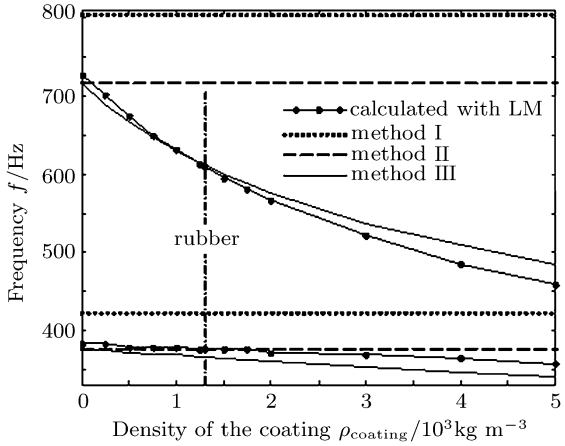


Fig.7. Frequencies on the edges of the lowest band gaps in the typical (a)2D and (b)3D ternary LR PCs at several densities of the coating material.

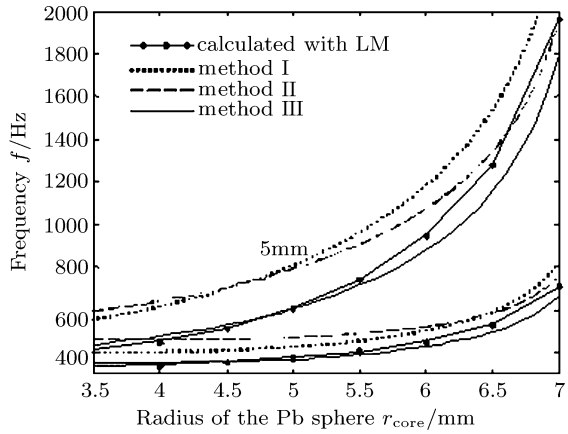


Fig.8. Frequencies on the edges of the lowest band gaps in the typical (a)2D and (b)3D ternary LR PCs at several radiuses of the core.

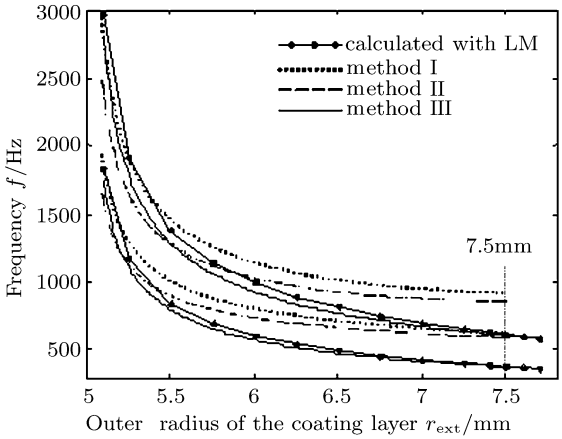


Fig.9. Frequencies on the edges of the lowest band gaps in the typical (a)2D and (b)3D ternary LR PCs at several outer radiuses of the coating layer.

From these figures, we can see that the frequencies evaluated with method I are higher than the theoretical ones, especially on the upper edge of the band gap. The analogous models with parameters calculated with method I match with the 2D and 3D LR PCs basically only on the lower edges of their band gaps. These mismatches are due to the underestimate of stiffness k, i.e. the equivalent stiffness of coating layer in region A in Fig.4. Hirsekorn's simplification, where the rubber is treated as a layer with an equal-thickness Δr, is not accurate because the thickness (along the direction of wave propagation) in the coating layer is Δr only at the centre of region A and longer than Δr at other parts in region A. In method II, we improve it by regarding each slender bar along the direction of wave propagation in region A as a tiny spring, and stiffness k as the sum of the stiffnesses of all these tiny springs in parallel connection. Thus, using the integral technique, we have the new effective stiffness k for 2D case as

$$k = 4C_{11}\int_0^{r_{\rm core}} \frac{{\rm d}x}{\sqrt{r_{\rm ext}^2-x^2}-\sqrt{r_{\rm core}^2-x^2}} = 2C_{11}\left[\frac{r_{\rm core}}{\sqrt{r_{\rm ext}^2-r_{\rm core}^2}} + \frac{\pi r_{\rm core}^2/2 + r_{\rm ext}^2 \arcsin(r_{\rm core}/r_{\rm ext})}{r_{\rm ext}^2-r_{\rm core}^2}\right], \tag{8}$$

and for the 3D case as

$$\begin{aligned} k &= 2C_{11}\int\!\!\int_{(x^2+y^2)\le r_{\rm core}^2} \frac{1}{\sqrt{r_{\rm ext}^2-x^2-y^2}-\sqrt{r_{\rm core}^2-x^2-y^2}}\,{\rm d}x{\rm d}y \\ &= 2C_{11}\int_0^{2\pi}\int_0^{r_{\rm core}} \frac{r{\rm d}r{\rm d}\theta}{\sqrt{r_{\rm ext}^2-r^2}-\sqrt{r_{\rm core}^2-r^2}} = \frac{4\pi C_{11}}{3(r_{\rm ext}^2-r_{\rm core}^2)}\left[r_{\rm ext}^3+r_{\rm core}^3-(r_{\rm ext}^2-r_{\rm core}^2)^{3/2}\right]. \end{aligned} \tag{9}$$

Using method II, we evaluate again the frequencies of the lowest band gaps in 2D and 3D ternary LR PCs with different structural and material parameters (dashed lines in Figs.5–9) and compare them with the calculated with the LM method (solid lines with dots in Figs.5–9).

We can see that the frequencies evaluated with method II are much more accurate than those evaluated with method I. However, there still exists a large mismatch according to the upper edges of the band gap. Especially in Fig.7, when the density of the coating layer changes, the evaluated frequencies should remain unchanged according to methods I and II while the actual values decrease obviously in the inverse proportion to the density. This is due to the fact that the density of coating layer is not taken into consideration in the calculation of parameters in models illustrated in Fig.3.

We can find that when the LR PCs vibrate as they are modelled in Fig.3(b) (on the upper edge of the band gap), there exists a standing point that is immovable in the corresponding vibration modes. Thus the mass of the coating layer in region A can be divided into two masses and they are added to m_1 and m_2 in Fig.3(b) respectively. Based on the detailed vibration modes illustrated in Fig.2, we can see that the coating layer in region B vibrates as the attachment of the host layer does, which means that the mass of region B can be added to m_2 directly. Thus in method III, the expressions for the calculation of m_1 and m_2 are changed into

$$\begin{aligned} m_1 &= m_{\rm core} + m_A\frac{\alpha}{1+\alpha}, \\ m_2 &= m_{\rm host} + m_B + m_A\frac{1}{1+\alpha}, \end{aligned} \tag{10}$$

where

$$\alpha = m_2/m_1 = \frac{m_A+m_B+m_{\rm host}}{m_A+m_{\rm core}}. \tag{11}$$

For the 2D case, the mass of the coating layer in region A and that in region B, respectively, are

$$m_A = \rho_{\text{coating}}\pi(r_{\text{ext}}^2 - r_{\text{core}}^2) - m_B,$$
$$m_B = 2\rho_{\text{coating}} \int_{r_{\text{core}}}^{r_{\text{ext}}} 2\sqrt{r_{\text{ext}}^2 - x^2}\, \mathrm{d}x = 2\rho_{\text{coating}} \left(\arccos(r_{\text{core}}/r_{\text{ext}}) r_{\text{ext}}^2 - r_{\text{core}} \sqrt{r_{\text{ext}}^2 - r_{\text{core}}^2} \right). \quad (12)$$

As for the 3D case, we have

$$m_A = \frac{4}{3}\rho_{\text{coating}}\pi(r_{\text{ext}}^3 - r_{\text{core}}^3) - m_B,$$
$$m_B = 2\rho_{\text{coating}} \int_0^{2\pi} \int_{r_{\text{core}}}^{r_{\text{ext}}} \sqrt{r_{\text{ext}}^2 - r^2} r \mathrm{d}r\mathrm{d}\theta$$
$$= \frac{4}{3}\rho_{\text{coating}}\pi(r_{\text{ext}}^2 - r_{\text{core}}^2)^{3/2}. \quad (13)$$

The frequencies evaluated with method III and illustrated as solid lines in Figs.5–9 match well with the theoretical results on both the upper and the lower edges of the LR band gaps.

As for the 2D ternary LR PCs, we can obtain similar conclusions. By using the method III, we can also evaluate the frequencies on both the lower and upper edges of the first band gaps of the 2D ternary LR PCs successfully.

4. Conclusions

The vibration modes on the lower and the upper edges of lowest band gaps of the ternary locally resonant phononic crystals can be described with the 'mass–spring–fixture' and the 'mass–spring–mass' models respectively. The parameters of the models are given in a reasonable way based on the physical insight into the band gap mechanism. The analytical estimations with the models and the theoretical predictions with the lumped-mass method are in good agreement with each other, especially for the upper edge of the locally resonant band gap. The proposals of these models are heuristic and helpful for a better understanding of the locally resonant band gap mechanism as well as accurate evaluation of the corresponding band edge frequencies. The latter makes it possible to make a simple design of locally resonant gaps in phononic crystals, which is important for their applications in low frequency vibration/noise shelters.

5. Acknowledgment

One of the authors, G. Wang, wishes to thank Mr M. Hirsekorn for his heuristic discussion. The authors would like to thank the anonymous referee for valuable comments and suggestions.

References

[1] Kushwaha M S, Halevi P, Dobrzynski L and Djafari-Rouhani B 1993 *Phys. Rev. Lett.* **71** 2022
[2] Liu Z, Zhang X, Mao Y, Zhu Y Y, Yang Z, Chan C T and Sheng P 2000 *Science* **289** 1734
[3] Martínez-Sala R, Sancho J, Sánchez J V, Gómez V, Llinares J and Meseguer F 1995 *Nature* (London) **378** 241
[4] Goffaux C, Sanchez-Dehesa J and Lambin P 2004 *Phys. Rev.* B **70** 184302
[5] Goffaux C and Sánchez-Dehesa J 2003 *Phys. Rev.* B **67** 144301
[6] Goffaux C, Sánchez-Dehesa J, Yeyati A L, Lambin P, Khelif A, Vasseur J O and Djafari-Rouhani B 2002 *Phys. Rev. Lett.* **88** 225502
[7] Hirsekorn M 2004 *Appl. Phys. Lett.* **84** 3364
[8] Hirsekorn M, Delsanto P P, Batra N K and Matic P 2004 *Ultrasonics* **42** 231
[9] Wen J H, Wang G, Liu Y Z and Yu D L 2004 *Acta Phys. Sin.* **53** 3384 (in Chinese)
[10] Wang G, Liu Y Z, Wen J H and Yu DL 2006 *Chin. Phys.* **15** 407
[11] Wang G, Wen J and Wen X 2005 *Phys. Rev.* B **71** 104302
[12] Wang G, Wen X, Wen J, Shao L and Liu Y 2004 *Phys. Rev. Lett.* **93** 154302
[13] Wang G, Wen J, Liu Y and Wen X 2004 *Phys. Rev.* B **69** 184302
[14] Cao Y, Hou Z and Liu Y 2004 *Phys. Lett.* A **327** 247
[15] Hua J, Zhang S and Cheng J C 2005 *Acta Phys. Sin.* **54** 1261 (in Chinese)
[16] Qin B, Chen J J and Cheng J C 2005 *Chin. Phys.* **14** 2522
[17] Yablonovitch E 1987 *Phys. Rev. Lett.* **58** 2059
[18] John S 1987 *Phys. Rev. Lett.* **58** 2486